January 2013

User-based filter utilization for multicarrier schemes

Zekeriyya Esat Ankarali
University of South Florida, zekeriyya@mail.usf.edu

User-based Filter Utilization for Multicarrier Schemes

by

Zekeriyya Esat Ankaralı

A thesis submitted in partial fulfillment
of the requirements for the degree of
Master of Science in Electrical Engineering
Department of Electrical Engineering
College of Engineering
University of South Florida

Major Professor: Hüseyin Arslan, Ph.D.
Richard D. Gitlin, Sc.D.
Thomas Weller, Ph.D.

Date of Approval:
November 1, 2013

Keywords: Intentional overlapping, Multiple accessing, Adaptive filtering, Multi-user scenarios, Roll-off factor

DEDICATION

To my dear parents;

Dr. Arif Ankarali and Fatma Ankarali,

and my dear siblings;

Sadullah, H. Abdulaziz and Erva.

ACKNOWLEDGMENTS

First, I extend my thanks to my God for everything that He granted me in this life. I would like to thank my advisor Dr. Hüseyin Arslan for his guidance, encouragement, and support throughout my study. I wish to thank Dr. Richard D. Gitlin and Dr. Thomas Weller for serving in my committee and for offering valuable suggestions. I also thank all the USF College of Engineering staff for their sincere assistance whenever I need.

It has been a great privilege to be a member of the Wireless Communications and Signal Processing (WCSP) group. This group did not only provide a perfect research environment with very valuable collaborations, but had me witness a real model of friendship. I would like to thank my friends Ali Görçin, Sadia Ahmed, Alphan Şahin, M. Bahadır Çelebi, Anas Tom, Murat Karabacak, M. Harun Yılmaz, Ertugrul Güvenkaya, Osman Şaylı, Ali Fatih Demir and Emre Seyyal for their support as friends and productive discussions as colleagues.

Special thanks to Ali Görçin for his sincere and continuous support with his precious life experiences, Alphan Şahin for long hours of fruitful discussions and collaboration during my master period, and Ertugrul Güvenkaya for his great assistance through the writing process of this thesis.

I wish to thank the members of my new family in law, Dr. Fatih Gultekin, Hediye Gultekin and their sons Muhammed Ali, Sadullah, Ismail Emir, and especially their dear daughter, my fiancee Amine for all the moral support and prayers throughout the last and maybe the most stressful period of this process.

Last, but by no means least, I would like to express my deepest gratitude to my parents Fatma Ankaralı, Dr. Arif Ankaralı, and my dear brothers Sadullah, H. Abdulaziz and my lovely sister Erva for their immense sacrifice and unconditional support throughout all these challenging years. I have never thanked them enough, but I want them to know that I am always grateful to the God for having such a family.

TABLE OF CONTENTS

LIST OF TABLES

LIST OF FIGURES

ABSTRACT

Multicarrier modulation is a transmission technique that is quite convenient for high data rates in wireless communication. Information symbols are partitioned and parallelly sent over multiple narrowband subchannels. Pulse shaping filters are critically important in multicarrier modulation for determining the characteristics of signal in time and frequency domains. In this thesis, we propose a new pulse shaping approach for multicarrier schemes to increase spectral efficiency in multi-user scenarios. Conventionally, the time-frequency lattice and the prototype filter are designed considering the worst-case of time-varying multipath channel. However, this approach ignores to make use of multi-user diversity and leads to excessive spacings between successive symbols in time and frequency. Unlike the prevalent methods, we investigate user-based filter utilization considering the wireless channel of each user individually to prevent over-design and improve spectral efficiency. Also, this approach is implemented in a denser time-frequency lattice design. Symbols are allowed to be overlapped (depending on time-frequency dispersion of their individual channels) as long as the signal-to-interference ratios (SIRs) observed by all users are kept above a certain level. Employing user-specific filters to enhance SIR of the user exposed to the most interference provides more overlapping flexibility. Therefore, further improvement in spectral efficiency is achieved in our wireless communication system design.

CHAPTER 1:

INTRODUCTION

Wireless communication systems has exhibited a great transition from voice-oriented services to data hungry multimedia applications, over the last two decades [1]. Especially, since the introduction of smart and mobile terminals into the market, number of wireless multimedia users has increased tremendously [2]. There is an explosive growth in demand for seamless connectivity and high data rates at anytime and anywhere. However, considering the scarcity in spectrum, accommodating these demands with conventional techniques is a challenging issue. Therefore, novel methods that provide high data rates by utilizing spectral resources efficiently are required.

Multicarrier modulation is a transmission scheme that is quite convenient for wireless broadband communication [3]. A general block diagram for multicarrier-based systems is given in Figure 1. Basically, transmission bandwidth is divided into N narrow sub-bands and the bit stream is partitioned into parallel sub-streams for each subchannel. In that way, data of each subchannel is transmitted with a lower rate, i.e., symbol duration, T is extended to $N \times T$. Therefore,

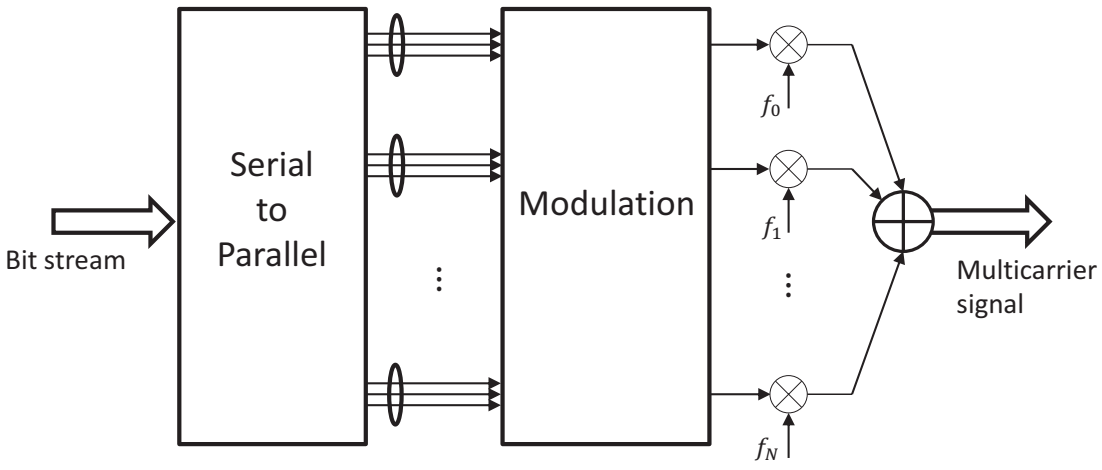

Figure 1.1 General block diagram for multicarrier-based systems

transmission becomes less sensitive to multipath delay spread. However, dividing the band into narrow subchannels increases the vulnerability of signal against the issues in frequency domain such as carrier frequency offset (CFO) and Doppler spread. Also, parallel transmission of independent symbols results in a signal with high peak-to-average power ratio (PAPR) that may cause in-band interference due to the non-linearity of power amplifiers (PA). Therefore, aforementioned facts should be considered carefully in designing multicarrier-based transmission systems. A more detailed discussion about multicarrier modulation is given in chapter 2.

Although the fundamental theory of multicarrier transmission has been existed since early sixties, it drew attention in the last two decades. Among the several multicarrier schemes, orthogonal frequency-division multiplexing (OFDM) is the most popular one so far. Because, OFDM exhibits very attractive features such as, fast implementation with fast Fourier transformation (FFT), trivial eqaulization with cyclic prefix (CP) and well adoption to multiple input-multiple output (MIMO) channels. With all of these advantages, OFDM has been employed in many standards. Very-high-speed Digital Subscriber Line-2 (VDSL-2) [6] and European standards Digital Audio Broadcasting (DAB) [4] and Terrestrial Digital Video Broadcasting (DVB-T) [5] are some of them using OFDM as the modulation method. Also several versions of Wireless Local Area Networks (WLAN) [7] are all developed based on OFDM. These versions are ETSI HiperLAN/2 by Europe, ARIB HiSWANa by Japan and the American standard IEEE 802.11a/g.

Although OFDM still keeps its popularity, there are several issues that OFDM may not easily overcome. As pulse shaping filter of OFDM can be considered as rectangular, its subcarriers have a shape of sinc function that has substantially large and infinitely long sidelobes. All of the aforementioned issues about OFDM arise from these sidelobes. For instance, adjacent spectrum of an OFDM signal that consists of many subcarriers cannot be used without guard bands. That is because sidelobes of these subcarriers are combined in the adjacent channels and create a significant interference. This is a challenge in employing OFDM in Cognitive Radio (CR) type of applications where secondary users should assure not to interfere with signals of primary users. In literature, many sidelobe suppression techniques are proposed such as filtering, windowing, and precoding. However, these techniques either reduce spectrum efficiency or introduce a large complexity. Additionally, OFDM is very sensitive to CFO caused by frequency misalignment between oscillators of

transmitter and receiver. Similarly, high mobility in the environment that corresponds to Doppler spread results in a degradation in performance.

One may note that, aforementioned issues of OFDM are related with delocalization of subcarriers since OFDM dictates only rectangular filter for pulse shaping. In this point, filter bank multicarrier (FBMC) techniques provide a good alternative by enabling transmission system to take the advantage of various filters. Therefore, the filter that has the best time and frequency characteristics according to the needs of transmission can be selected.

FBMC was firstly introduced as a multicarrier technique for real-valued symbol transmission by Chang in 1966. Then, in [9] Saltzberg showed how this technique can be used to transmit complex-valued symbols, i.e., quadrature amplitude modulation (QAM) symbols. In-phase and quadrature components of QAM symbols are modulated with sine and cosine waves separately. In order to avoid interference between symbols, proper filters shaping the pulses in time and frequency are employed and perfect reconstruction was achieved by using the proper filter at the receiver. Also, fast implementation was carried out by polyphase structure, proposed in [16]. Until today, three modes of FBMC has been presented in the literature, cosine-modulated multitone (CMT), staggered multitone (SMT) and filtered multitone (FMT). Unlike CMT and SMT, symbols are not overlapped in FMT which makes it less efficient in spectrum. However, FMT is very convenient for MIMO, in contrast to other modes.

As a matter of fact, environments of wireless users may not have identical characteristics, even if they are served by the same base station (BS). A group of users who are stationary and very close to the BS may have a non-dispersive channel and an excellent received power. However, another group who are far away from the BS and driving in a downtown area may receive a weak and dispersed signal in time and frequency. Although some user-based approaches exist such as power control, adaptive modulation and coding in conventional methods, waveform design is the same for all the users. For example, a prototype filter is used for pulse shaping of all symbols in an FBMC-based transmission. If multipath delay spread is the major concern about the channel, then prototype filter is designed considering the user whose channel is the most dispersive in time. However, such a procedure likely results in a degradation in spectrum efficiency.

In order to present a more specific explanation, let the prototype filter be root-raised cosine (RRC) filter. Basically, sidelobes of RRC filter in time domain constitute the main threat in time dispersive channels [30]. Therefore, sidelobes should be suppressed considering the most dispersive state of the channels in time. However, such an over protection is not required for the users whose signals do not experience that much dispersion. Then, employing a prototype filter leads to an unnecessary bandwidth usage as sidelobe suppression in RRC corresponds to widening of occupied bandwidth. Unlike conventional waveform design techniques, if user specific filters are utilized by evaluating the environment of each user individually, overdesign can be prevented and required bandwidth for the same data rate can be decreased. However, difference between user-specific filters may cause loss of orthogonality and introduce an additional interference to the transmission. In Chapter 3[1], this extra interference is investigated for RRC filters. Also, a procedure estimating the required bandwidth for the maximum allowable interference, i.e., desired signal-to-interference ratio (SIR) is provided. In order to present this study, FMT mode of FBMC is selected as the case study because of its simple structure.

Orthogonality of symbols in time and frequency domain is the most important criterion to avoid inter-carrier interference (ICI) and inter-symbol interference (ISI), and conventional multi-carrier schemes are designed in accordance with that. However, maintaining orthogonality may not be a major concern in some cases. For example, if noise constitutes the dominant effect in transmission, some interference negligible to noise may be allowed. In such cases, keeping orthogonality limits the efficiency of spectrum utilization. Introducing controlled overlapping between symbols in time and frequency may provide the same data rate by using less spectral resource. In Chapter 4[2], a denser frame structure that consist of intentionally-overlapped symbols is proposed. FMT is selected as the case study and RRC filter is used for pulse shaping as in Chapter 3. Although similar approaches exist in literature, previously explained multi-user diversity is also exploited in proposed technique to provide more overlapping flexibility. This is carried out by performing channel estimation for each user and assigning user-based filters that maximize the SIR of the user

[1]This work is published in [27].
[2]This work is published in [28].

in the worst case, respectively. Then, symbols are overlapped in time and frequency unless the interference on the user in the worst case exceed the allowable level.

1.1 Organization of Thesis

This thesis consists of five chapters. An overview to multicarrier modulation is provided in Chapter 2. In Chapter 3, adaptive usage of roll off factor in multicarrier communication systems is introduced. A simple design procedure is also given at the end of the chapter. Then, an intentional overlapping technique for multicarrier schemes based on user specific filter design is presented in Chapter 4. In order to achieve desired SIR performance with minimum bandwidth occupation filters are designed considering the medium of each user. Numerical results are also given at the end of the chapter. Finally, Chapter 5 concludes the thesis with a general discussion and future studies related with proposed techniques.

CHAPTER 2:

AN OVERVIEW TO MULTICARRIER MODULATION

2.1 Introduction

In this chapter various aspects of multicarrier modulation are introduced. After explaining general system model, a comparison between multicarrier modulation and single carrier modulation in terms of the main impairments in wireless communication is provided.

2.2 System Model

Multicarrier modulation corresponds to data transmission in multiple streams through different frequencies. Instead of sending the information symbols back to back expeditiously, multiple symbols are transmitted simultaneously in parallel. Therefore, a multicarrier symbol consists of many information symbols with a longer duration as compared to a single carrier symbol which consists of only one information symbol. Analytical expression of a multicarrier signal can be given as,

$$x(t) = \sum_{m=-\infty}^{\infty} \sum_{k=0}^{N-1} X_{mk} p\left(t - mT\right) e^{j2\pi kFt} \ , \tag{2.1}$$

where N is the number of subcarriers, X_{mk} is the complex symbol located on the subcarrier indicated by the time index m, and the frequency index k, T is the symbol spacing, F is the subcarrier spacing, and $p\left(t\right)$ is the prototype pulse shaping filter.

After the signal passes through the linear time-varying wireless channel $h(t, \tau)$, the received signal is obtained as

$$y(t) = \int_{-\infty}^{\infty} h(t, \tau) x(t - \tau) d\tau \ . \tag{2.2}$$

Received symbol $\tilde{X}_{nl}$ located on time index n and frequency index l is obtained by the projection of the received signal on analysis function $\acute{g}_{nl}(t)$ as

$$\tilde{X}_{nl} = \langle y(t), \acute{g}_{nl}(t) \rangle, \tag{2.3}$$

where

$$\acute{g}_{nl}(t) = p\left(t - nT\right) e^{j2\pi lFt}, \tag{2.4}$$

and $\tilde{X}_{nl}$ in (2.3) indicates the estimated symbol.

2.3 Multicarrier Modulation versus Single Carrier

As the advantages of each scheme come with their trade-offs, it is not proper to claim that any scheme is totally better than the others. It totally depends on the medium and the evaluation criteria. Therefore, multicarrier and single carrier schemes should be discussed and compared in more specific aspects.

2.3.1 Performance in Time Dispersive Channels

Wireless signal, sent from transmitter is spread over the medium and each component reaches the receiver through different paths by reflecting from the objects in the environment. Although, all components are combined in the receiver, their arrivals may occur with different delays depending on lengths of their ways. This effect is called multipath delay spread and these kind of channels are named as time dispersive channels.

In time domain point of view, delayed multipath components of a symbol arrive at the receiver at the same time with later symbols and contribute them. This occurrence is called inter-symbol interference (ISI). Single carrier systems are more sensitive to this effect than multicarrier systems. Because, for a given number of symbols and bandwidth, symbols are sent serially and faster in single carrier systems while they are sent in parallel through a longer time duration in multicarrier-based transmission. Therefore, the ratio of the maximum access delay of channel

impulse response (CIR) to the symbol duration becomes much less in multicarrier systems as illustrated in Figure 2.1.

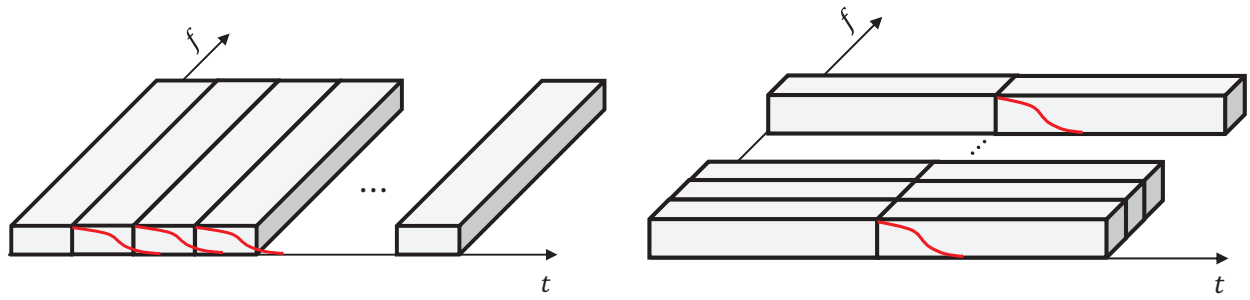

(a) Single carrier (b) Multicarrier

Figure 2.1 Illustration of delay spread in single carrier and multicarrier systems

Time dispersive channels becomes selective in frequency domain, i.e., channel gains vary according to frequency. As a result of this selectivity, channel may have deep fadings in some frequency ranges. In frequency domain equalization of a signal after passing through a frequency selective channel, signal is multiplied by the inverse function of channel gains. However, before equalization, noise addition occurs at the receiver. Since, inverse function of the channel takes large values in deeply fading frequencies to equalize the signal, noise is highly enhanced in these frequencies.

In single carrier systems, highly enhanced noise is a serious problem. Because, even if it is locally enhanced in frequency, inverse Fourier transform spreads that local noise though the whole symbols in time domain and that may result in misdetection of many symbols. On the other hand, in multicarrier systems, total bandwidth is partitioned into subcarriers in such a way that channel of each subcarrier becomes nearly flat, i.e., channel gain in frequency does not vary within the band of any subcarrier. The maximum bandwidth that satisfy this is called coherence bandwidth. Unless the bandwidth of subcarriers is determined broader than coherence bandwidth, noise enhancement damages only the subcarrier localized in the corresponding frequency. Therefore, multicarrier systems are said to be more robust against frequency selective channels.

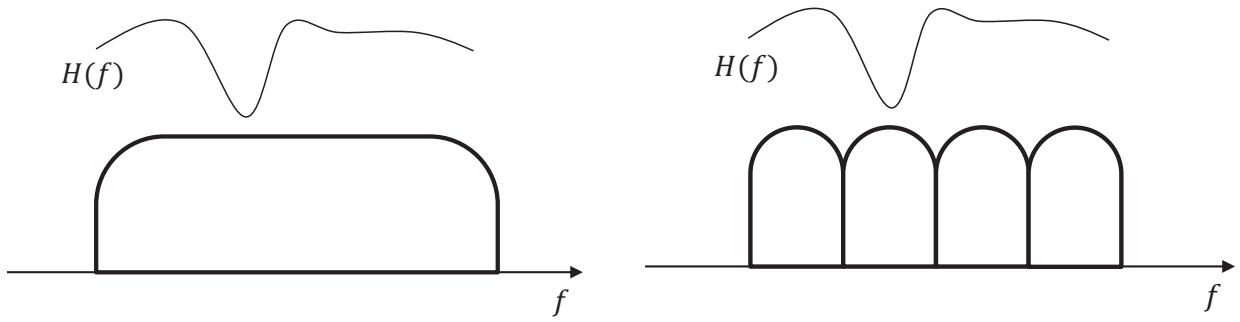

(a) Single carrier (b) Multicarrier

Figure 2.2 Illustration of frequency selective channels for single carrier and multicarrier systems

2.3.2 Performance in Frequency Dispersive Channels

Electromagnetic waves shift in frequency when the source has a relative velocity to the receiver different than zero. This phenomenon is called Doppler shift. If many signals that encounter different Doppler shifts are combined at the receiver, it ends up with a spread signal in frequency. This phenomenon is called Doppler spread and the channels effecting wireless signals in that way are called frequency dispersive channels.

In a mobile environment, each subcarrier of a multicarrier signal undergoes frequency dispersion. Therefore, if there is not a guard band between subcarriers, Doppler spread results in inter-carrier interference (ICI) in multicarrier systems. On the other hand, since bandwidth is not divided into subbands in single carrier systems, they can be said more robust against frequency dispersive channels.

2.3.3 Peak to Average Power Ratio (PAPR)

In wireless communication high peak-to-average power ratio (PAPR) is a major drawback of wireless signal, $x(t)$, defined as

$$PAPR(x(t)) = \frac{max\{|x(t)|^2\}}{\mathrm{E}[|x(t)|^2]} \tag{2.5}$$

where E[.] is expectation operator and $x(t)$ is assumed zero mean.

Due to the nonlinear characteristic of power amplifier (PA), a signal with high PAPR likely does not fit the dynamic range of PA. Therefore, after passing through the PA, signal components exceeding the dynamic range of PA are scaled differently or directly clipped. This effect causes in-band interference and signal faces a substantial distortion.

2.3.4 Carrier Frequency Offset (CFO)

Conveying a signal from baseband to the radio frequency (RF) at the transmitter and down-converting an RF signal to the baseband at the receiver is carried out by local oscillators. Carrier frequency offset (CFO) is another hardware based impairment that occurs due to the frequency misalignment of local oscillators in transmitter and receiver. If it is not estimated and compensated properly, signal encounters a shift in frequency and each subcarrier gets contribution from its adjacent channel. This contribution can be considered as ICI and cause a serious degradation in signal quality.

CHAPTER 3:

ADAPTIVE ROLL-OFF FACTOR UTILIZATION IN FILTERED MULTITONE (FMT) BURST STRUCTURES

3.1 Introduction

Consistently increasing number of users along with wide variety of wireless communication applications, and extensive growth of the user demands from the wireless communication systems require more adaptive, flexible, and efficient future radio access techniques. Especially, over the last two decades, radio access techniques which are able to exploit the multidimensional electrospace, e.g. orthogonal frequency-division multiplexing (OFDM), have been heavily investigated in the literature.

Recently, filter bank multicarrier (FBMC) technique which was introduced by Chang and Saltzberg in 1960s [9, 10], is re-considered as a tempting solution for future radio access technologies because of its flexibility on pulse shapes along with filters well-localized in frequency. Basically, the flexibility of choosing any prototype filter makes FBMC an attractive choice over OFDM.

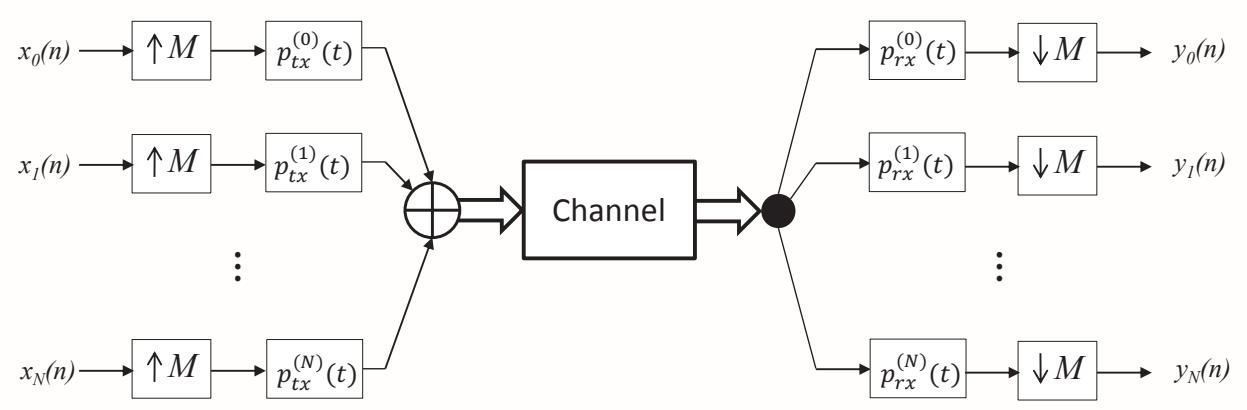

Figure 3.1 General block diagram of FMT

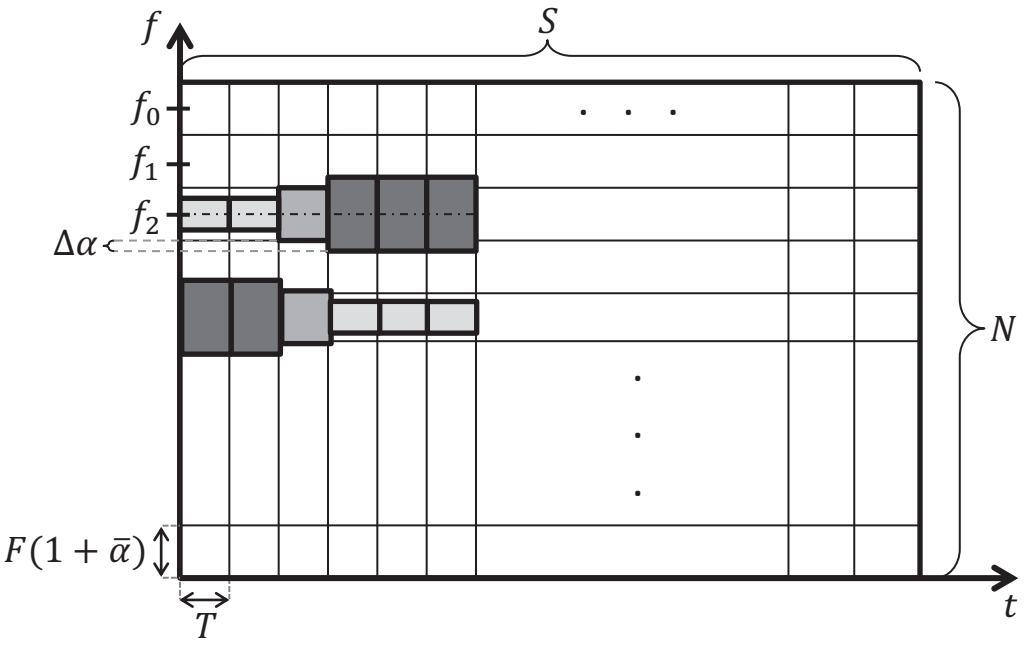

Figure 3.2 Proposed burst structure.

It is possible to generate FBMC symbols with different modes, i.e., filtered multitone (FMT), staggered multitone (SMT), and cosine-modulated multitone (CMT) [11]. FMT-based FBMC whose block diagram is given in Figure 3.1 is a multicarrier scheme that has been proposed for DSL applications [12, 13]. In this mode, subcarriers are separated with guard bands instead of overlapping of adjacent subcarriers as in SMT and CMT modes. Therefore, FMT-based FBMC does not provide the same efficiency of SMT and CMT modes because of guard bands. However, FMT brings flexibility on multiple input-multiple output (MIMO) channels which makes an attractive scheme for next generation communications systems.

In FBMC, time and frequency characteristics of transmitting and receiving filters are the critically important for the system performance. For example, consider an FBMC symbol generated with root-raised cosine (RRC) filter. Basically, roll-off factor (α) determines the time and frequency characteristics of RRC filter. If small α is applied to the filter, higher sidelobes are obtained in time domain and makes the constructed FMT-based FBMC symbols more susceptible to time varying channels.

In the literature, existing methods are based on designing prototype filter to achieve better sidelobe suppression for perfect reconstruction [15, 17]. In [18], the effects of roll-off factor and

truncation are also analyzed. These methods are useful when only a single prototype filter is applied for whole burst structure. However, use of fixed α factors ignores the adaptations on time-frequency varying channels. In this study, instead of using single prototype filter for the whole burst, α value is changed by $\pm\Delta\alpha$ for the consecutive FBMC symbol by paying regard to the orthogonality loss due to the change on α as given in Figure 4.1. Therefore, desired α on each subcarrier is obtained by changing α factor gradually within the range between α_{min} and α_{max} specified according to transmission quality requirements. In addition to α adaptation, interference between subcarriers is allowed in the proposed burst structure. Frequency spacing, which is directly to related with inter-carrier interference (ICI), is determined according to an average $\bar{\alpha}$ factor as $F(1+\bar{\alpha})$. The main contributions of proposed method are given as follows:

1. Different α values are applied to the burst structure. Therefore, instead of using single prototype function, advantage of controlling the filter in time and frequency domains is utilized in the burst structure.

2. By allowing controlled interference, new degree of freedoms, i.e., $\bar{\alpha}$, $\Delta\alpha$, and truncation are introduced and investigated.

This chapter is organized as follows: FMT-based FBMC system modeling is presented in Section 3.2. In Section 3.3, orthogonality of the burst structure is analyzed considering different parameters, i.e., $\bar{\alpha}$, $\Delta\alpha$, and filter length. Then, corresponding burst designing procedure is explained. Finally, simulation results are given by using the proposed burst structure.

3.2 System Model

Analytical expression of the FMT-based baseband transmitted signal can be given by

$$x(t) = \sum_{m=-\infty}^{\infty} \sum_{k=0}^{N-1} X_{mk} p\left(t - mT\right) e^{j2\pi kFt} \ , \tag{3.1}$$

where N is the number of subcarriers, X_{mk} is the complex symbol located on the subcarrier indicated by the time index m, and the frequency index k, T is the symbol spacing, F is the subcarrier spacing, and $p\left(t\right)$ is the RRC prototype filter as

$$p\left(t\right)=$$

$$\begin{cases} 1-\alpha_{mk}+4\frac{\alpha}{\pi}, & t=0 \\ \frac{\alpha}{\sqrt{2}}\left[\left(1+\frac{2}{\pi}\right)\sin\left(\frac{\pi}{4\alpha}\right)+\left(1-\frac{2}{\pi}\right)\cos\left(\frac{\pi}{4\alpha}\right)\right], & t=\pm\frac{T}{4\alpha} \\ \frac{\sin\left((1-\alpha)\frac{\pi t}{T}\right)+\frac{4\alpha t}{T}\cos\left((1+\alpha)\frac{\pi t}{T}\right)}{\frac{\pi t}{T}\left(1-\frac{16\alpha^2t^2}{T^2}\right)}, & |t|\leq T_{\mathrm{f}} \\ 0 & \text{otherwise} \end{cases} \tag{3.2}$$

where T_{f} is filter duration as $T_{\mathrm{f}}=KT$ and K is the filter length as a multiple of symbol spacing. In FMT mode, in order satisfy the orthogonality, F has to be selected at least as $F=\frac{1}{T}(1+\bar{\alpha})$ if $K=\infty$.

After the signal passes through the linear time-varying wireless channel $h(t,\tau)$, the received signal is obtained as

$$y(t)=\int_{-\infty}^{\infty}h(t,\tau)x(t-\tau)d\tau\ . \tag{3.3}$$

Received symbol $\tilde{X}_{nl}$ located on time index n and frequency index l is obtained by the projection of the received signal on analysis function $\acute{g}_{nl}(t)$ as

$$\tilde{X}_{nl}=\langle y(t),\acute{g}_{nl}(t)\rangle, \tag{3.4}$$

where

$$\acute{g}_{nl}(t)=p\left(t-nT\right)e^{j2\pi lFt}. \tag{3.5}$$

In (3.4), $\tilde{X}_{nl}$ indicates the estimated symbol.

3.3 Designing Burst Structure

Time-frequency characteristics of RRC filter is determined by α as mentioned before. Also, since RRC has an infinite length in time, it is truncated in practical systems. This truncation also effects the characteristic of the filter in both domain. Therefore, we investigate these parameters before designing the burst structure.

3.3.1 Truncation (K) and Roll-Off Factor (α) in RRC Filter

RRC filter is one of the most well-known pulse shaping filters in wireless communication. Basically, it is obtained by taking the root of raised cosine (RC) filter in frequency domain, as its name implies. The main reason of dividing one filter into two filters, i.e., using two RRC filters instead of one RC filter is performing match filtering that improves signal-to-noise ratio (SNR) of received signal in the transmission. Symbols, filtered with RRC at the transmitter, are filtered with RRC at the receiver again. Therefore, transmission ends up with RC filtered pulses which are orthogonal to each other. Time-frequency characteristics of RRC filters are determined by α which can take value between 0 and 1. As α increases, sidelobes of the filter in time domain are suppressed. However, filter occupies a larger band in frequency proportional to α. In Figure 3.3, α effect is shown for both domain.

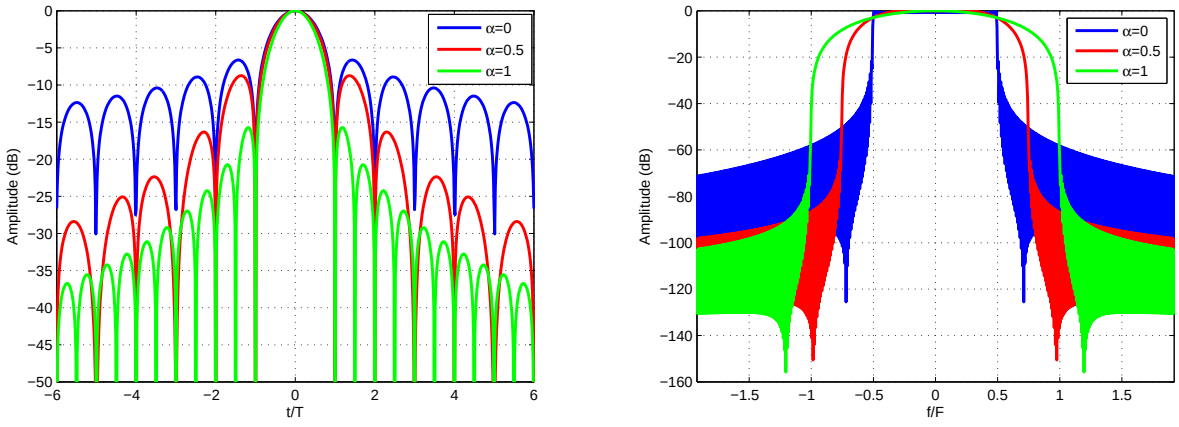

(a) (b)

Figure 3.3 Effect of α on filter sidelobes and bandwidth

Ideally, RRC filters are infinite impulse response (IIR) filters and their convolution can satisfy Nyquist criterion only in that case. However, generating longer filters introduce more complexity and it cannot be infinite for practical cases. Therefore, RRC filters are truncated in implementation. This leads to some changes in filter characteristic as shown in Figure 3.4. Truncation corrupts orthogonality by shifting zero crossing points of RC filter in time domain. Also, some of in-band energy leak to the out of band in frequency domain which causes adjacent-channel interference (ACI).

In Figure 3.5, combined effect of filter length, K determined by truncation and α is provided. Since both parameters have an important effect on signal-to-interference ratio (SIR) performance, their selection should be done carefully considering the desired performance and complexity.

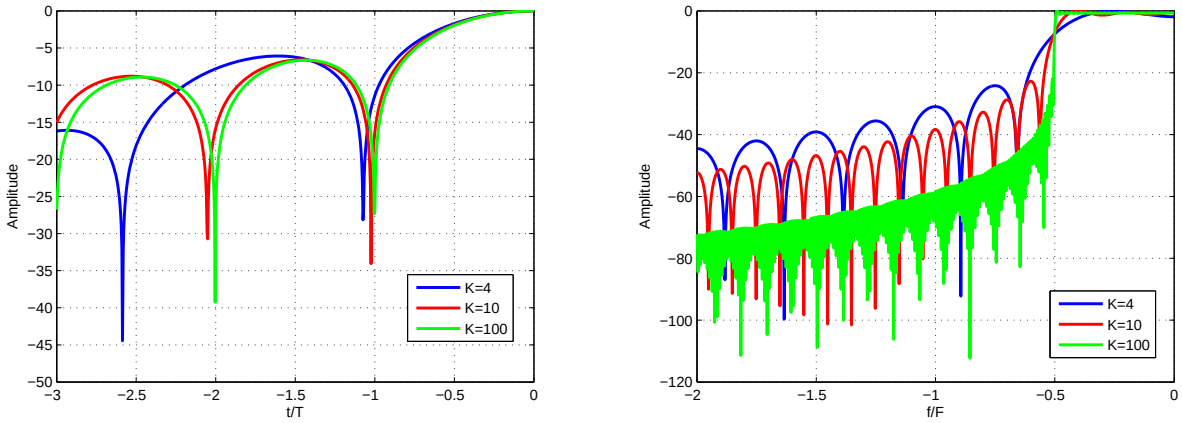

(a) (b)

Figure 3.4 Effect of filter length (truncation) on filter in time and frequency

3.3.2 Design Procedure

Another issue resulting in orthogonality loss within the proposed frame structure is employing different α_{mk} for different symbols. In conventional approaches, a single prototype filter is used for all symbols at the transmitter and receiver. Therefore, the information symbols are decoded at receiver based on Nyquist criterion if filter truncation and channel effect are excluded. However, since the proposed technique introduces an adaptive burst structure with α_{mk} for each m and k, orthogonality is lost between adjacent symbols in time and frequency domain. In addition to that,

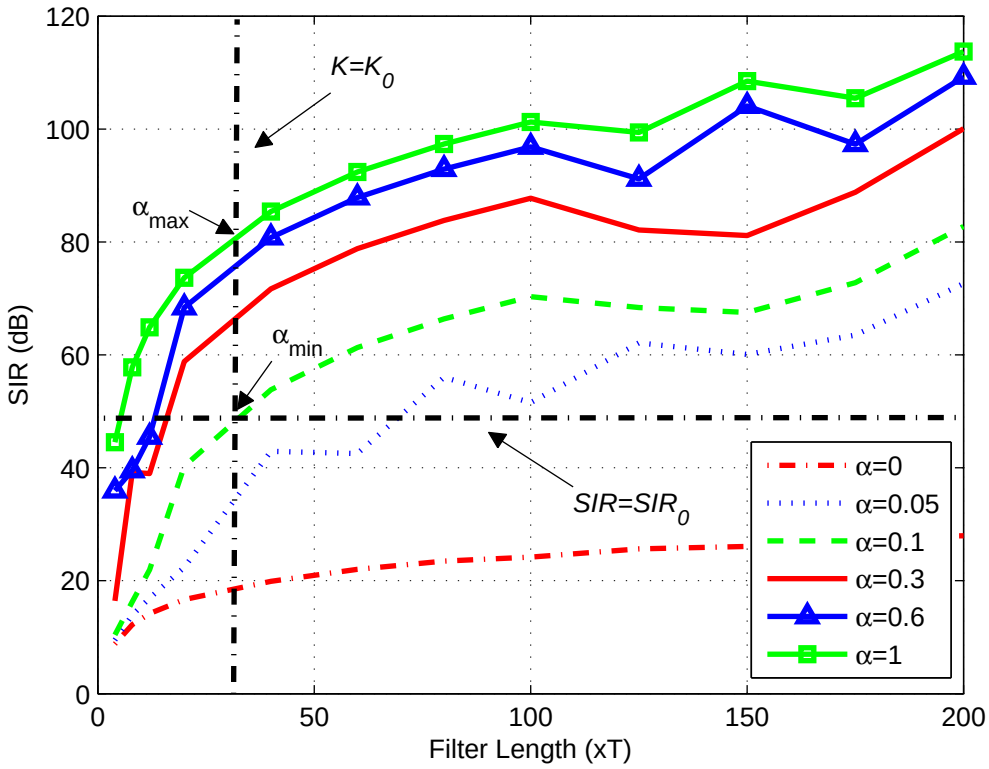

Figure 3.5 The impact of truncation on SIR for different α.

even if the transmitter and receiver filters are matched, the tails of adjacent symbols that have different α_{mk} values spoil the perfect reconstruction. Thus, in order to limit the interference due to the tails of different α_{mk}, the variation of the α_{mk} factor for the consecutive symbols is limited and gradually changed with $\mp\Delta\alpha$. As shown in Figure 3.6, the smoother transitions in α_{mk} also result in smoother SIR changes. On the contrary, the sharp transitions in α_{mk} cause more interference and larger variation of SIR.

Under these circumstances, three main parameters, K, $\bar{\alpha}$ and $\Delta\alpha$, are critically important to maintain SIR above a minimum value, $SIR \geq SIR_{min}$. In addition, α_{min} and α_{max} must be specified by considering the orthogonality loss. First, in order to see the effect of K, SIR curves are given in Figure 3.5 for different α_{mk} and K. Figure 3.5 provides a selection space to specify α_{min} by showing the limitations of system with two lines pointing to the maximum filter length that can be generated by the hardware and minimum desired SIR which are indicated by K_0 and SIR_0.

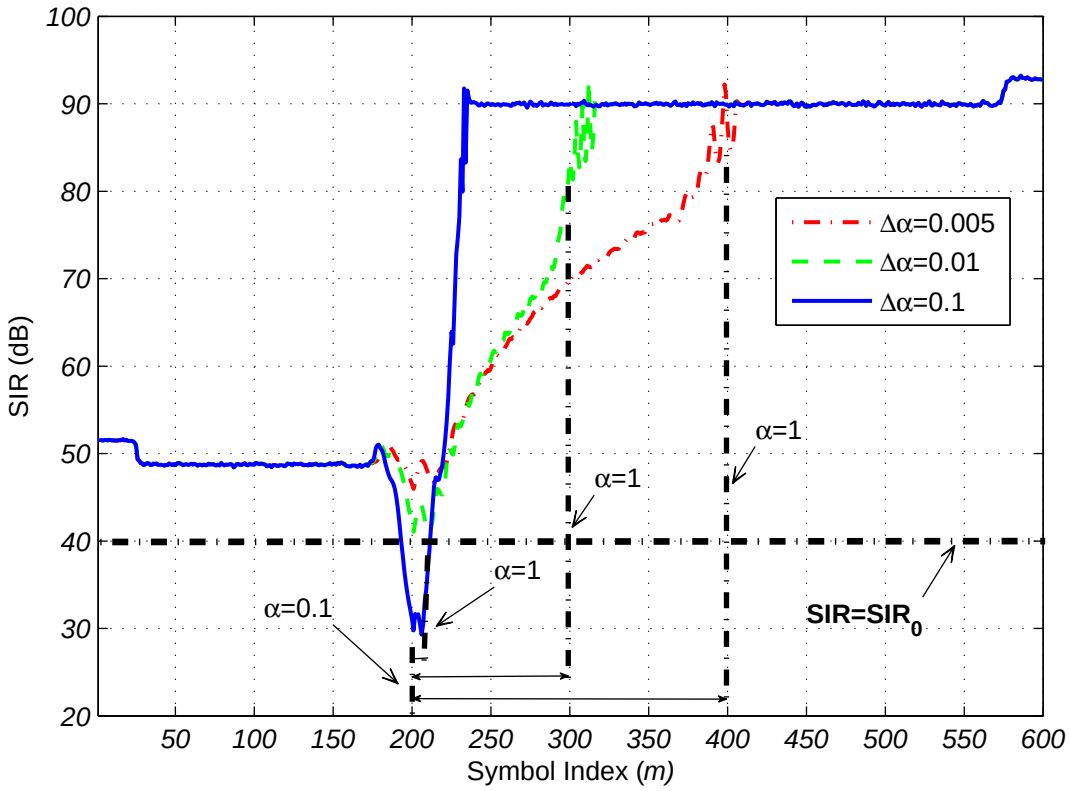

Figure 3.6 The impact of $\Delta\alpha$ on instantaneous SIR in the burst structure ($K = 40$).

Since there are other impairments except truncation impact, a margin must be left on SIR_{min} to determine the adaptation space on α_{mk}. Thus, SIR_0 indicates (SIR_{min}+SIR_{margin}). Then, $\Delta\alpha$ is determined as the second main parameter. The impact of $\Delta\alpha$ on SIR is obtained in Figure 3.6 using the greatest transition in terms of α_{mk} variation from predetermined α_{min} to α_{max} for different $\Delta\alpha$. Channel dispersion quantity and SIR_0 specify α_{min} and α_{max}. For example, α_{min} and α_{max} are set to 0.1 and 1 in Figure 3.6, respectively. Note that faster changes in α causes high SIR degradation but quick SIR compensation in time.

The final step to complete the proposed design structure is to determine $\bar{\alpha}$. In Figure 3.7, SIR is calculated for different α_{mk} for given $\bar{\alpha}$. Note, each curve is constructed for bursts whose all symbols have corresponding α_{mk} value. However, in real implementations, α_{mk} takes random values between α_{min}-α_{max}. Therefore, if α_{max} and the probability density function (PDF) of α_{mk} ($f_\alpha(\alpha)$) in the system are known, minimum required $\bar{\alpha}$ can be obtained by calculating the expected

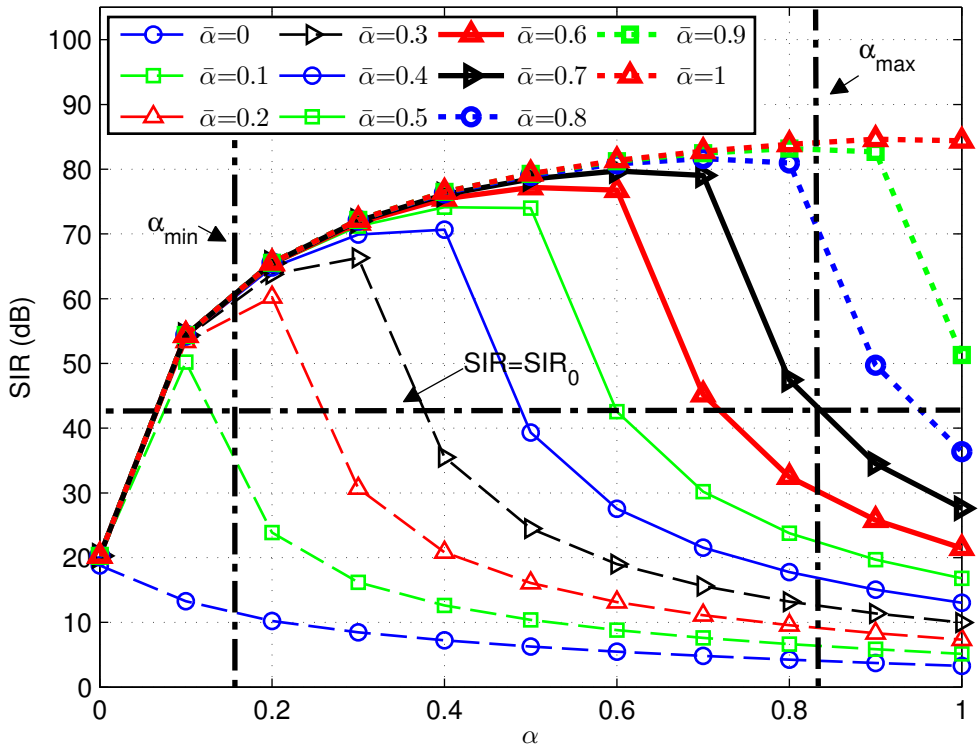

Figure 3.7 The impact of $\bar{\alpha}$ on SIR for different α.

SIR value of each curve ($\overline{SIR}(\bar{\alpha})$) in Figure 3.7 as

$$\bar{\alpha}_{min} = \arg\min_{\bar{\alpha}} \left(\left| \overline{SIR}(\bar{\alpha}) - SIR_0 \right| \right) . \tag{3.6}$$

where

$$\overline{SIR}(\bar{\alpha}) = 10 \log \left(\int_{\alpha_{min}}^{\alpha_{max}} 10^{\frac{SIR_{\bar{\alpha}}(\alpha)}{10}} f_\alpha(\alpha) d\alpha \right) . \tag{3.7}$$

In (3.7), $\overline{SIR}(\bar{\alpha})$ and $SIR_{\bar{\alpha}}(\alpha)$ indicate the average SIR for a given $f_\alpha(\alpha)$, SIR for given α and $\bar{\alpha}$ as in Figure 3.7, respectively.

When all of the required parameters are determined properly, the adaptive burst structure satisfying SIR_0 requirement with minimum bandwidth can be designed.

3.4 Simulations

A design example is given in order to verify described procedure with computer simulations and to investigate the performance of the proposed burst structure. The burst is designed with 330 FBMC symbols and 16 subcarriers. Roll off factor of each subcarrier's symbols vary for 3 times. The transmission quality requirement, i.e., SIR_0, is selected as 40 dB. If the maximum filter length K_0 is assumed as 40 because of the hardware limitations, as shown in Figure 3.5, α_{min} needs to be larger than 0.1 and α_{max} can be selected as 1 without any constraint. On the other hand, $\Delta\alpha$ is determined 0.01 to keep the SIR more than 40 dB using Figure 3.6. If PDF of α_{mk} is assumed as uniform heuristically, $\bar{\alpha}$ is calculated as 0.65 using (3.6). When the burst is designed with these parameters, average SIR is obtained as 47.8 dB which satisfies desired transmission quality. For different SIR_0 values, a list of determined parameters and measured SIR values are given in Table 3.4 ($\alpha_{max} = 1$, $\Delta\alpha = 0.01$).

Table 3.1 Simulation results for different SIR_0 values ($\alpha_{max} = 1$, $\Delta\alpha = 0.01$).

SIR_0 (Theoretical)	α_{min}	$\bar{\alpha}$	SIR (Simulation)
20 dB	0.05	0.35	23.4 dB
30 dB	0.05	0.55	39.8 dB
50 dB	0.2	0.75	57.4 dB

3.5 Concluding Remarks

In this chapter, an adaptive FMT based FBMC burst structure is proposed to compensate the impairments of doubly dispersive channels to maintain SIR. Roll off factors of the symbols in the proposed burst are changing adaptively within an α range specified according to transmission requirement. Also, subcarriers are allowed to be overlapped considering for a given SIR level. By employing the proposed burst structure, the spectral efficiency of the burst is increased by adjusting the subcarrier spacing according to the PDF of the roll-off in the system, instead of adjusting for the worst case. By introducing α adaptation and partially overlapping between subcarriers by maintaining SIR, new degree of freedoms in the burst structure are achieved. Especially, if the introduced degree of freedoms can be exploited with scheduling algorithms and adaptive modula-

tion to yield better proposed structure. As an extension of this chapter, the statistics of roll-off considering the channels of the users and the impact of scheduling on proposed burst structure can be discussed.

CHAPTER 4:

INTENTIONAL-OVERLAPPING FOR MULTICARRIER SCHEMES BASED ON USER-SPECIFIC FILTERS

4.1 Introduction

Increasing data rate demand leads wireless community to develop new signaling schemes that improve spectral efficiency. Conventional multicarrier schemes aim to achieve this by avoiding inter-carrier interference (ICI) and inter-symbol interference (ISI). Therefore, Nyquist criterion which corresponds to locating symbols orthogonal to each other, has been considered in the design of these systems [9, 10]. However, one of the major limitations that prevents increasing spectral efficiency in conventional systems is the minimum distance between neighboring symbols in time and frequency, set by Nyquist criterion. Also, in some cases, pushing system to keep orthogonality may be unnecessary. For example, if noise is the dominant effect on performance degradation as compared to ICI and ISI, a Nyquist based system design may lead to overdesign. At this point, one can raise an important question: *For a given data rate, is it possible to decrease the minimum distance between neighboring symbols in time and frequency less than specified by Nyquist criterion to increase spectrum efficiency?* In the literature, this issue was firstly investigated as faster-than-Nyquist (FTN) signaling by Mazo and examined what can enable communication to have faster data transmission while satisfactory bit-error rate (BER) performance is still maintained [20]. Results show that 25% more data rate than indicated by Nyquist can be achieved by keeping the minimum Euclidean distance between signals for sinc pulse. In some later studies, FTN was generalized to other filters and further improvements in data rate are obtained. In [21] and [22], this approach is extended by allowing ICI and ISI in multicarrier schemes and it is shown that packing the symbols in both dimensions, i.e., time and frequency, provides more spectral efficiency than one dimensional signaling.

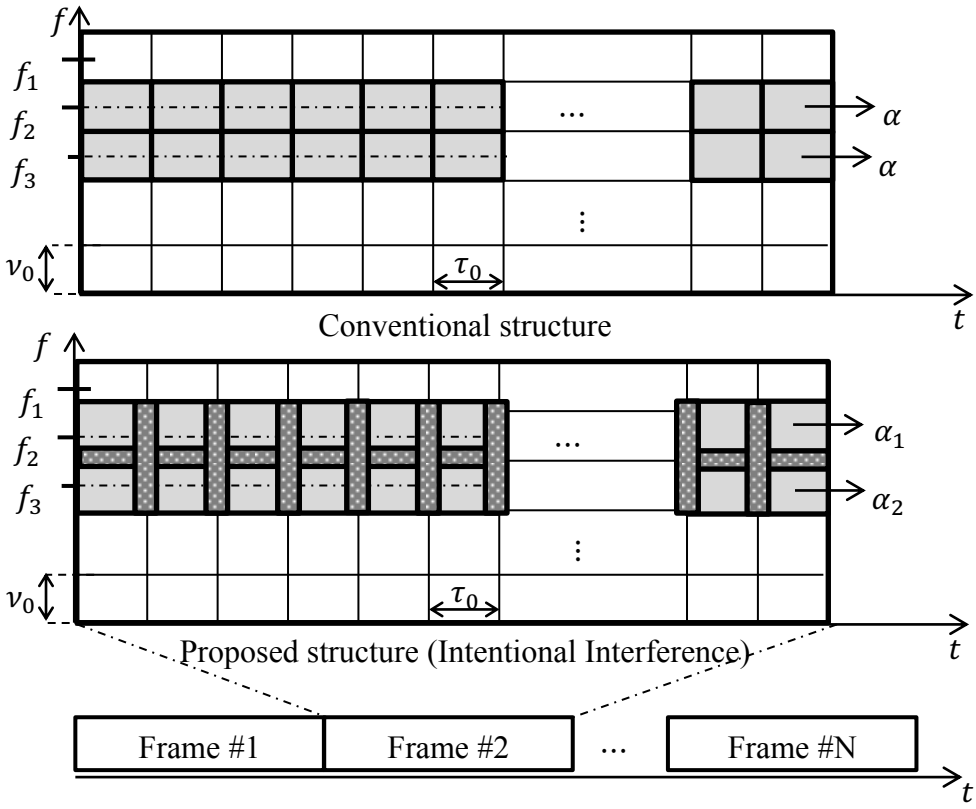

Figure 4.1 Conventional and proposed multicarrier structures.

Apart from these information theoretic approaches, partially overlapping (PO) techniques that consider not only the waveform but also the network have been proposed in literature [23]. In [24], a systematic model for PO is presented and shown that a careful usage of overlapped channels can significantly improve spectrum utilization. In [25], the maximum possible improvement with PO is studied. According to the investigations more flexibility in resource allocation is gained and overall network capacity can be increased by 100% as compared to conventional design. Channel allocation and link scheduling algorithms in MAC layer for partially overlapped channels are also proposed in [26].

Although existing studies in the direction of denser time-frequency structure enhance bandwidth utilization, they ignore the facts of multiuser scenarios, e.g., different distances between users and base station, mobility of the users, variety of the used applications. In this chapter, we propose a multicarrier approach which introduces intentional overlapping between successive symbols in time and frequency domain by taking the advantage of multi-user diversity in order to achieve

more spectral efficiency as shown in Figure 4.1. In multi-user scenarios, users can be assumed to have different channels in terms of dispersion in time and frequency. While a user stationary and very close to the base station may have a non-dispersive channel, another user driving in an urban area may suffer from a highly selective channel in time and frequency. In order to keep all users above a desired signal-to-interference ratio (SIR), conventional systems take precautions by considering the user in the worst case and design the whole system correspondingly. Note that, in this study, the user in the worst case indicates the user whose channel is the most dispersive in time and frequency, and all users are assumed to have the same requirement in terms of SIR. In a similar way, if an intentional overlapping is introduced to increase spectrum efficiency, the user in the worst case determines the maximum amount of overlapping between symbols. However, while this approach preserves all the users, it results in an over-designed system. Because, users in good case, i.e., users who have a low dispersive channel are unnecessarily protected as well, which degrades system efficiency. In order to prevent overdesign and achieve the same data rate with less bandwidth, user-based precautions are considered in [27]. These precautions are based on pulse shape filtering in this study. Therefore, rather than a fixed prototype filter, user specific filters are utilized to provide more overlapping flexibility.

In order to present the proposed technique, filtered multitone (FMT) in [12, 13] is selected as the case study, since it has a simple structure in time-frequency plane. Also, root-raised cosine (RRC) filter is used for the pulse shaping. Note that, this approach can also be performed with other type of filters. The parameter making filter specific to the user is roll-off factor (α) which determines time-frequency characteristic of RRC filters. Basically, channel estimation is performed for each user and proper user-specific filters that maximize the SIR of the users in worst case are assigned respectively. Then, symbols in burst structure are overlapped in time and frequency unless the SIR of the user in the worst case falls below a certain level. Note that, the time intervals or frequency spacings between successive symbols are the same in any case. However, overlapping amount between symbols may differ because of user-specific filter utilization. The main contributions of proposed method are given as follows:

- SIR requirement of users can be met by using less bandwidth as compared to the conventional approaches with single prototype filters. Alternatively, for a given bandwidth, overall SIR can be improved.

- Robustness against time-varying channel dispersions can be maintained with different filter adaptations by considering each user's channel individually.

This chapter is organized as follows: system model is given in Section 2. In Section 3, proposed scheme design procedure and construction of optimization problem are presented. Finally, numerical results are discussed in Section 4 and the chapter is concluded with Section 5.

4.2 System Model

4.2.1 Users

In this study, we focus on the downlink of the network where a base station serves M users indexed by i. Also, statistical characteristics of user channels are assumed independent.

4.2.2 Signaling

Analytical expression of the baseband transmitted signal with N subcarriers can be given by

$$x(t) = \sum_{m=-\infty}^{\infty} \sum_{k=-\frac{N}{2}}^{\frac{N}{2}-1} X_{mk} g_{mk}(t) \ , \tag{4.1}$$

where $g_{mk}(t) = p_{m,k}\left(t - m\tau_0\right) e^{j2\pi k\nu_0\tau_0}$, $p_{m,k}\left(t\right)$ is the synthesis filter utilized at the time index m and the frequency index k, X_{mk} is the complex symbol located on the subcarrier indicated by the time index m and the frequency index k, τ_0 and ν_0 the symbol spacing and subcarrier spacing, respectively. Assuming linear time-varying wireless channel, the received signal is expressed as

$$y_i(t) = \int_{\tau} \int_{\nu} H_i(\tau, \nu) x(t - \tau) e^{j2\pi\nu t} d\nu d\tau \tag{4.2}$$

where $H_i(\tau,\nu)$ is the Fourier transform of the channel impulse response of ith user. Also, the statistical characteristics of the channel is described with wide-sense stationary uncorrelated scattering (WSSUS) assumption given by

$$\mathrm{E}\left[H_i(\tau,\nu)\right] = 0 \ , \tag{4.3}$$

$$\mathrm{E}\left[H_i(\tau,\nu)H_i^*(\tau_1,\nu_1)\right] = S_i\left(\tau,\nu\right)\delta(\tau-\tau_1)\delta(\nu-\nu_1) \ , \tag{4.4}$$

where $S(\tau,\nu)$ is the channel scattering function.

At the receiver of user i, the symbol $\tilde{X}_{nl}$ located on time index n and frequency index l is obtained by the projection of the received signal on analysis function $\acute{g}_{nl}(t)$ as

$$\begin{aligned}\langle y_i(t), \acute{g}_{nl}(t)\rangle &\triangleq \int_t y_i(t)\acute{g}_{nl}^*(t)\mathrm{dt} \\ &= X_{nl}H_{nlnl} + \sum_{(m,k)\neq(n,l)} X_{mk}H_{nlmk} \ ,\end{aligned} \tag{4.5}$$

and

$$H_{nlmk} = \int_\tau\int_\nu H_i(\tau,\nu)\int_t g_{mk}(t-\tau)\acute{g}_{nl}^*(t)e^{j2\pi\nu t}\mathrm{dt}\mathrm{d}\nu\mathrm{d}\tau \ , \tag{4.6}$$

which captures the interference from the symbol (m,k) to the desired symbol (n,l). Similar to the transmitter, different analysis filters $\acute{p}_{n,l}\left(t-n\tau_0\right)$ are utilized at the receiver as $\acute{g}_{nl}(t) = \acute{p}_{n,l}\left(t-n\tau_0\right)e^{j2\pi l\nu_0 t}$.

4.2.3 Signal-to-Interference Ratio

If transmitted symbols, X_{mk} are assumed as independent identically distributed with zero mean and $\langle p_{m,k}\left(t\right), \acute{p}_{m,k}\left(t\right)\rangle = 1$, the power of desired part and the power of interference from

other symbols are obtained as

$$\sigma^2_{\mathrm{S},i} = \int_\tau \int_\nu S_i(\tau,\nu) \left|A(\tau,\nu)\right|^2 \mathrm{d}\nu\mathrm{d}\tau \ , \tag{4.7}$$

$$\sigma^2_{\mathrm{I},i} = \sum_{(m,k)\neq(0,0)} \int_\tau \int_\nu S_i(\tau,\nu) \left|A(m\tau_0+\tau, k\nu_0+\nu)\right|^2 \mathrm{d}\nu\mathrm{d}\tau \ , \tag{4.8}$$

respectively, where $\mathrm{E}[\cdot]$ is the expected value operator and $A(\phi,\psi)$ is the modified ambiguity function given as

$$A(\phi,\psi) \triangleq e^{-j2\pi\rho} \int_{-\infty}^{\infty} p_{m,k}(t-\phi)\, p^*_{\mathrm{rx}}(t)\, e^{j2\pi\psi t}\mathrm{d}t \ , \tag{4.9}$$

and $\rho = k\nu_0\tau$ [29]. Then, SIR of the ith user is obtained as $\gamma_i = \sigma^2_{\mathrm{S},i}/\sigma^2_{\mathrm{I},i}$. Minimum attainable SIR level in the system is denoted by $\gamma_{\min}$.

4.3 User-Specific Filter

For the sake of clarity, in this study, we consider an FMT based multicarrier structure in which symbols are shaped by RRC filters whose ambiguity function is given in Figure 4.2. Note that the same analysis can be performed for other type of filters [29]. The time-frequency characteristic of RRC filters is determined by roll-off factor. If a small α is applied to the filter, higher sidelobes are obtained in time domain which makes the symbols more susceptible to time dispersive channels [30]. On the other hand, increasing α results in a wider bandwidth and lower sidelobes. We associate each user with one subcarrier and a user-specific roll-off factor (α_i). Also, we assume that only one user utilizes the corresponding subcarrier in the frame.

Let Λ and Γ be vectors for the users-specific roll-off factors and corresponding SIRs as $\Lambda = [\alpha_1, \alpha_2, ..., \alpha_M]^T$ and $\Gamma = [\gamma_1, \gamma_2, ..., \gamma_M]^T$, respectively. Note that SIR is a function of not only ν_0, τ_0, and $H_i(\tau,\nu)$ but also Λ. Figure 4.3 may provide a better understanding for the effect of roll-off on SIR performance. There is no overlapping between the subcarriers and each curve is plotted for a fixed channel where τ_{rms} indicates root-mean-square (RMS) delay spread of exponentially decaying channel and symbol time, T is assumed as 1/15 ms. Length of RRC filter is also determined as $40T$. One may note that the curves don't linearly increase for the α values between 0 and 0.1.

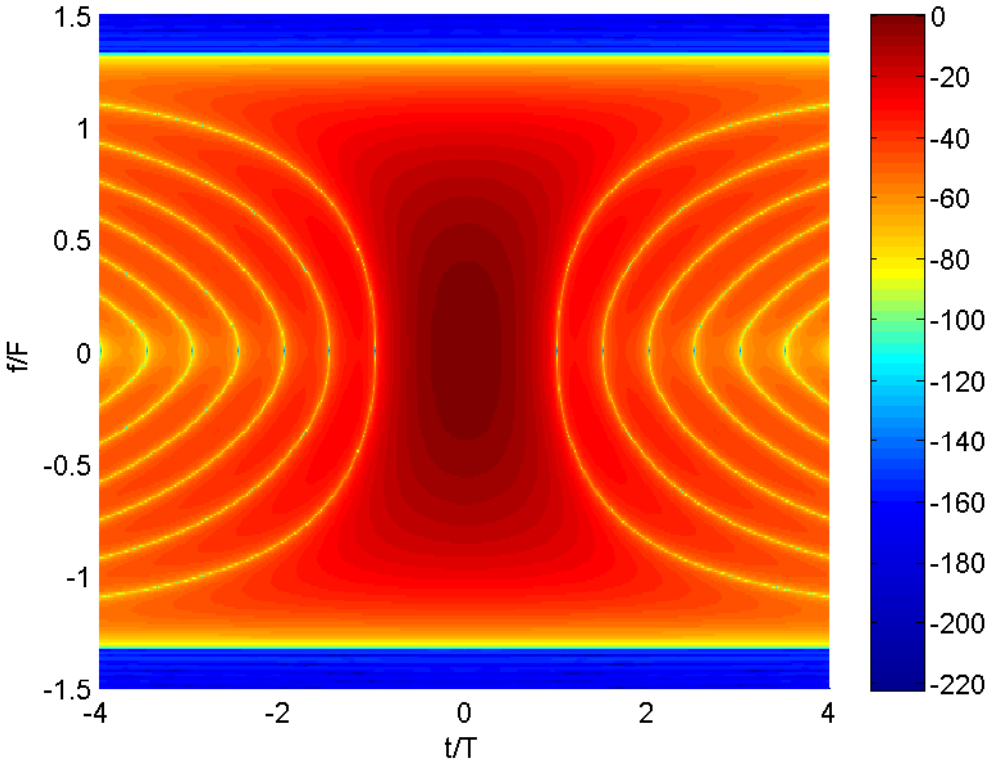

Figure 4.2 Ambiguity function diagram of RRC filter with $\alpha = 1$.

According to our investigation, this is caused by the truncation of RRC filter which has ideally an infinite impulse response (IIR). For that reason, more linear curves are obtained in Figure 4.4 where filter length is specified as $500T$. Since sidelobes of the filter are suppressed with increasing α, filter becomes more robust against time dispersive channel effect. Therefore, it can be assumed that the users whose channels are more dispersive in time are expected to have greater α values to keep their SIR on a certain level. This can also be interpreted as users in the worst case require more bandwidth. In order to make use of this fact and provide an extra space for intentional subcarrier overlapping, α-based scheduling is also considered. If α_i adjustment is done to maximize the SIR performance of the worst case users, overlapping limits can be extended as we target. Therefore, we jointly find the optimum user based α set to reach maximum possible overlapping.

In this study, our main objective function is minimizing the product of $\tau_0\nu_0$ for a given minimum $\gamma_{\min}$ and $H_i(\tau, \nu)$. However, this objective function requires an inverse function which

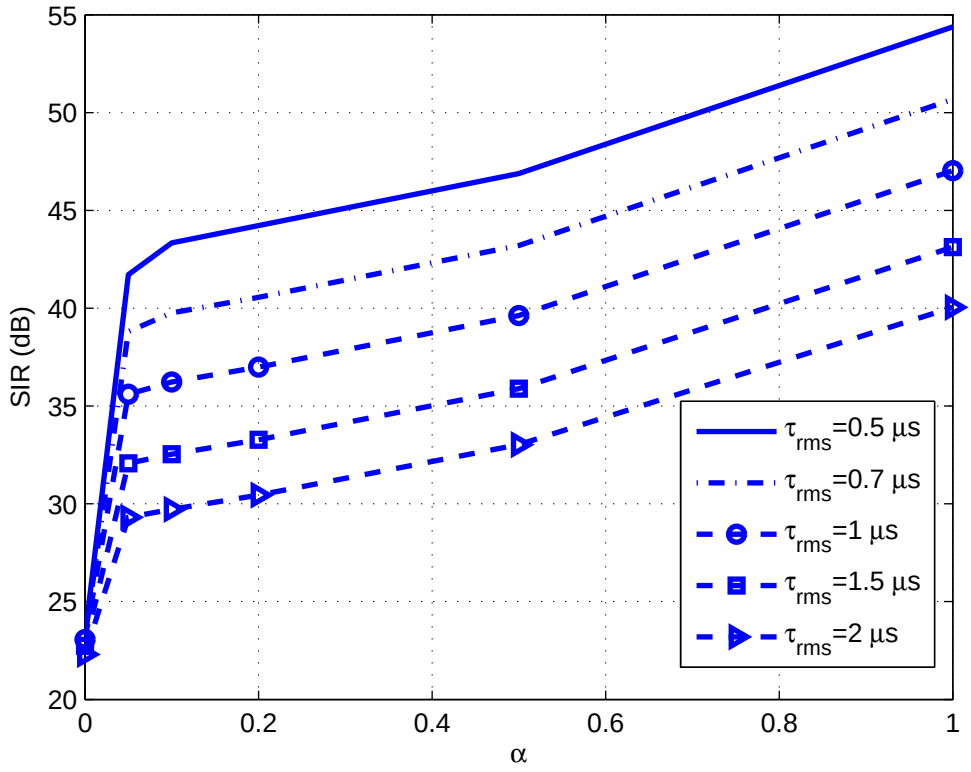

Figure 4.3 The impact of α on SIR in exponentially decaying channel with different τ_{rms} values ($K = 40T$).

yields $\tau_0\nu_0$ for given SIR and its derivation might be intractable. Instead, we follow another objective function given by

$$\Lambda = \arg\max_{\Lambda}\{\min(\Gamma)\} \tag{4.10}$$

$$\text{subject to } 0 \leq \Lambda < 1$$

for given τ_0 and ν_0. Note that, (4.10) indicates to maximize the SIR of the user in worst case by finding optimum roll-off factors for a given time interval and frequency spacing. In other words, for a given data rate, we calculate the optimum roll-off set maximizing SIR of the user in worst case. Therefore, although bandwidths of subcarriers change due to filter modification with roll-off factors, data rate is not affected by optimization.

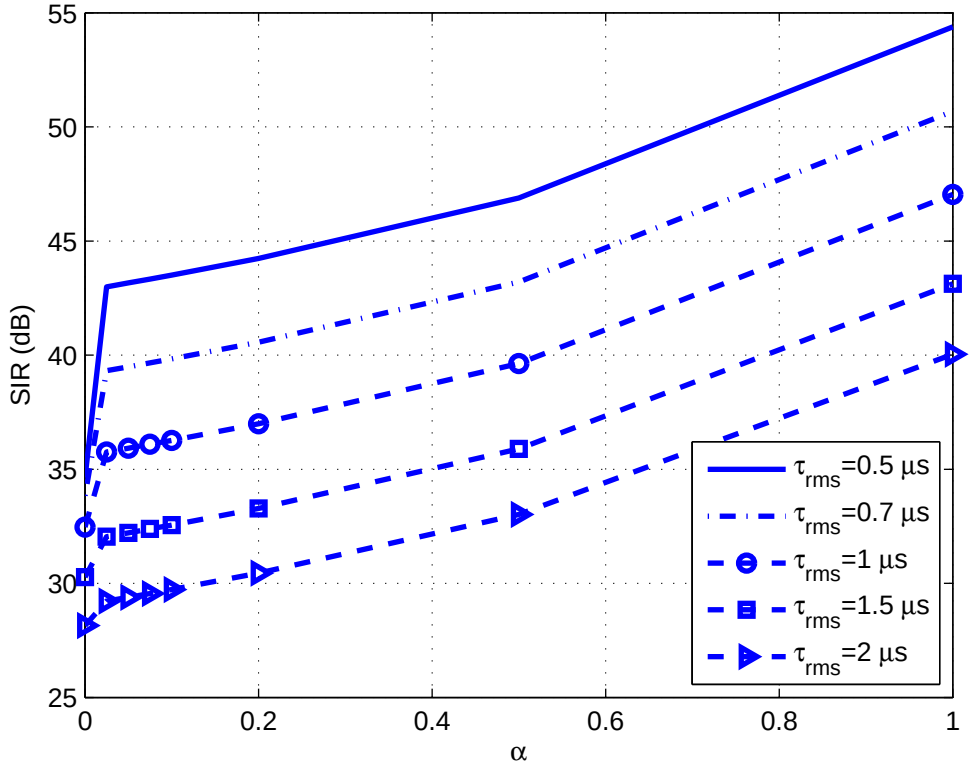

Figure 4.4 The impact of α on SIR in exponentially decaying channel for different τ_{rms} values ($K = 500T$).

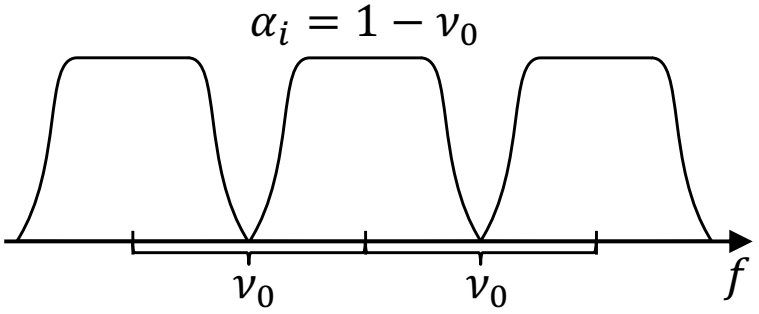

Figure 4.5 Illustration of non-overlapping subcarriers

Since this operation includes a nonlinear function as in (4.6), it corresponds to nonlinear least square problem, which is solvable with numerical methods, e.g., Levenberg-Marquardt [31]. When optimum Λ is obtained with (4.10), a table which includes the minimum SIR levels is constructed to select best $\tau_0\nu_0$ product.

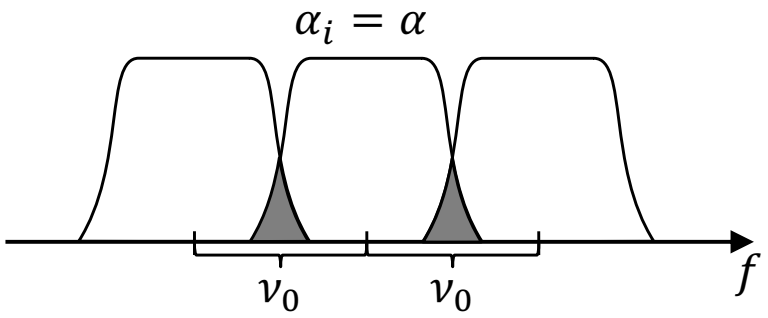

Figure 4.6 Illustration of fixed overlapping subcarriers

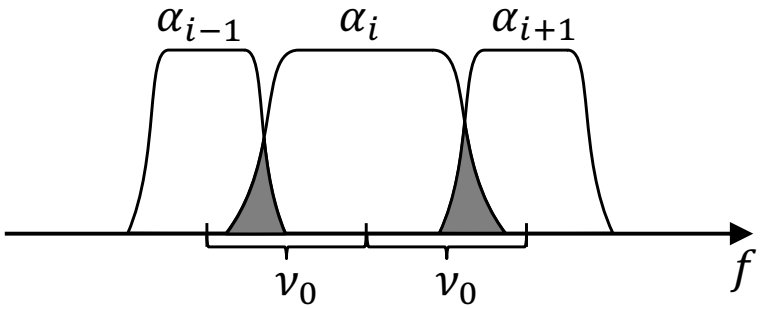

Figure 4.7 Illustration of user-based overlapping subcarriers

Considering (4.10), following transmission scenarios can be investigated:

- No Overlapping (NO): This is the conventional approach for FMT design. It does not introduce any overlapping in time and frequency domain as shown in Figure 4.3. The roll-off factor associated with the prototype filter is determined according to subcarrier spacing.

- Fixed Overlapping (FO): This approach allows overlapping between subcarriers. It introduces a trade-off between adjacent channel interference and the interference due to the time-varying channel. While increasing α provides more robustness against the multipath delay spread, it causes overlapping with neighboring symbols. However, the same α is used for all subcarriers, i.e., overlapping is fixed for all subcarriers as illustrated in Figure 4.3.

- User-Based Overlapping (UBO): This approach is the main focus of this paper. Unlike FO, it allows exploitation of user diversity to increase the spectral efficiency. While spacings are the same for all subcarriers, user specific filters in terms of α are utilized as shown in Figure 4.3

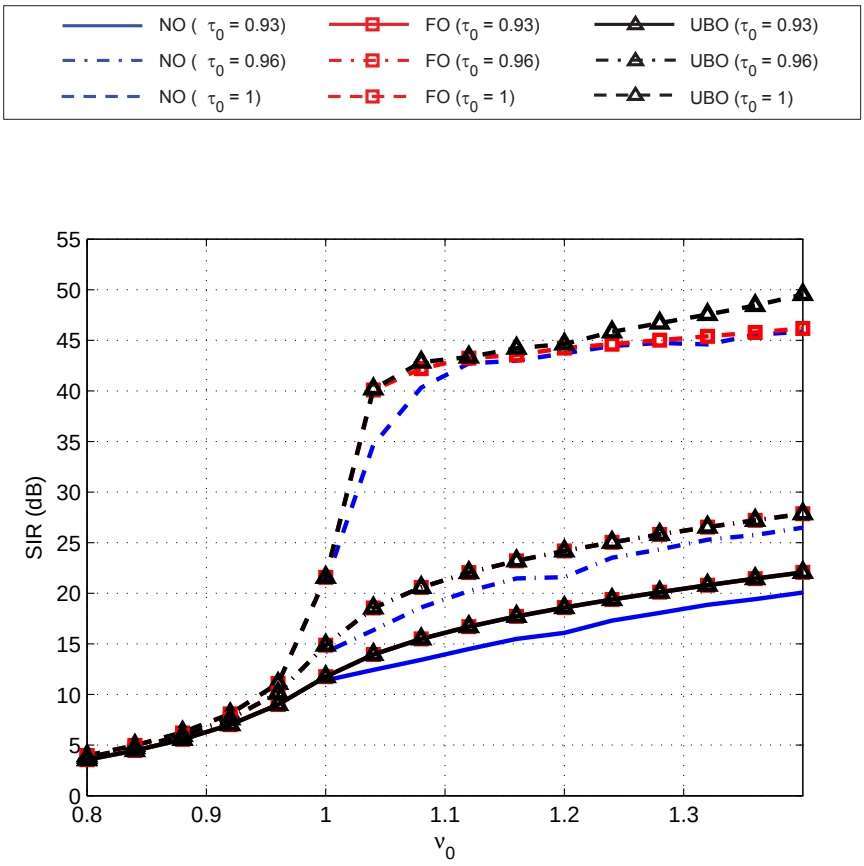

Figure 4.8 Achievable maximum $\gamma_{\min}$ results of NO, FO and UBO techniques under exponentially decaying multipath channel with $\tau_{\text{rms}} = 0.5$ μs.

to provide more overlapping flexibility. Note that, difference between overlapping amounts is caused by the different α

In the following section, ν_0, τ_0, and Λ are theoretically investigated for given communication medium.

4.4 Numerical Results

Performance of the proposed technique is evaluated and compared with the other approaches in this section. A multi-user scenario is realized where users are assumed to have different channels in terms of multipath delay spread and operate at different subcarriers. Number of subcarriers which equals to number of users, is determined as $M = 4$ where bandwidth of each subcarrier is

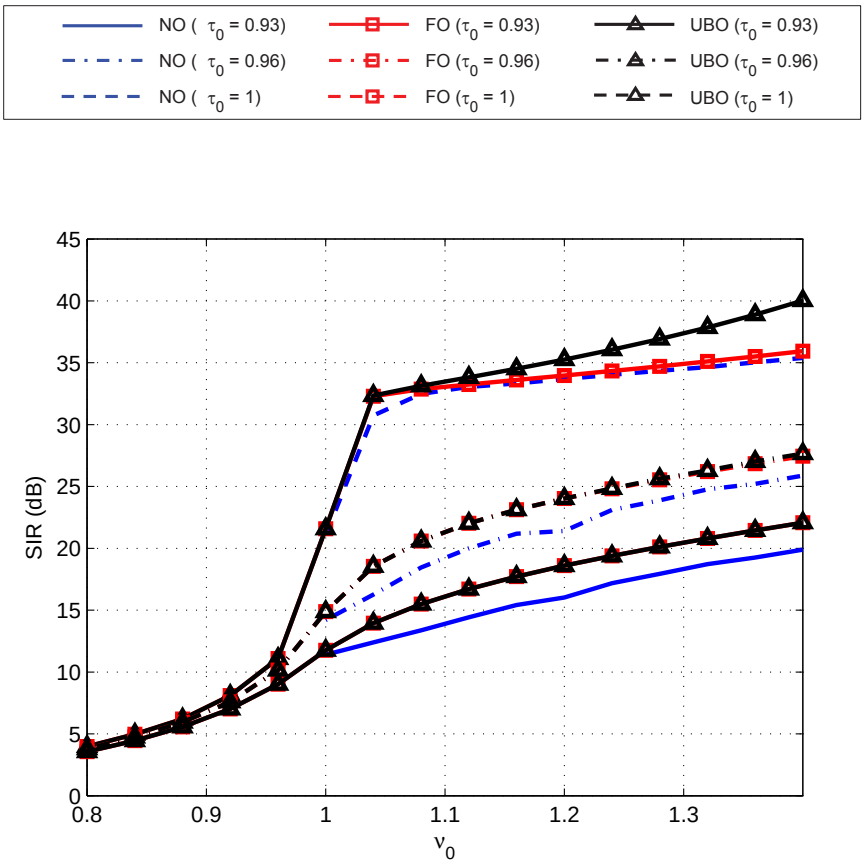

Figure 4.9 Achievable maximum $\gamma_{\min}$ results of NO, FO and UBO techniques under exponentially decaying multipath channel with $\tau_{\text{rms}} = 1$ μs.

selected $F = \frac{1}{T}$ =15 kHz as reference. Also, length of the RRC filter is chosen as $40T$. Performance of the three different techniques are presented under the effect of exponentially decaying channel. In order to reconstruct received data, a simple equalizer is performed which multiplies the received signal by a phase and amplitude correction factor based on complex channel taps. In order to determine phase-amplitude correction factor, we add a training sequence assumed to be known by the receiver to the signal before transmission. No interference cancellation mechanism is employed at the receiver. If we include such a functionality in our system, the proposed method would provide an additional improvement in BER performance.

Optimization problem given in (4.10) is solved with Levenberg-Marquardt algorithm. Note, this algoritm provides a local minimum of the input function. As our goal is maximizing min(Γ),

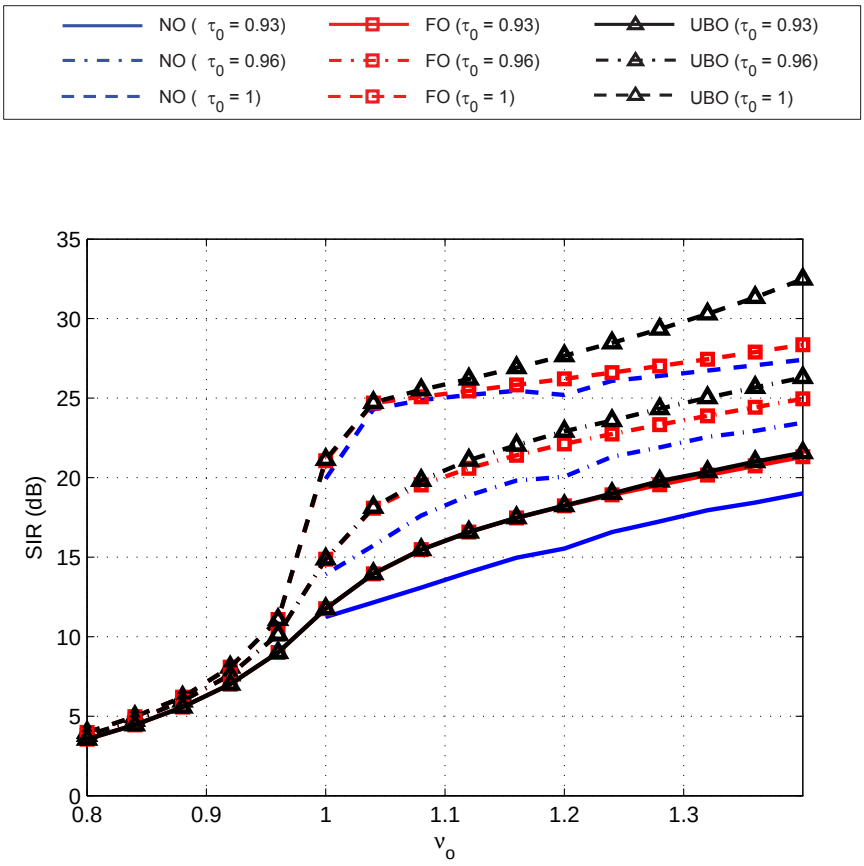

Figure 4.10 Achievable maximum $\gamma_{\min}$ results of NO, FO and UBO techniques under exponentially decaying multipath channel with $\tau_{\text{rms}} = 2$ μs.

input function is defined as

$$e = S_T - \min(\Gamma), \tag{4.11}$$

where S_T is a user defined target SIR, given as 50 dB for our case.

Since RRC filters are well localized in frequency and robust against Doppler spread, only multipath effect is considered. SIR performance of the user in the worst case, are given in Figure 4.10 for each technique with different τ_0 and ν_0 values. Note that, Figure 4.10 also implicitly provides the minimum required τ_0 and ν_0, whose product $\tau_0\nu_0$ corresponds to spectrum efficiency, for a given minimum desired SIR. In each figure, three τ_{rms} values are specified as 0.5 μs, 1 μs and 2 μs for the channel of worst case user and the channels of other users are assumed to be uniformly

Table 4.1 Required τ_0, ν_0 and α values for UBO and FO when $\gamma_{\min} = 22$ dB and $\tau_{\text{rms}} = 2$ μs.

(a)

User (FO)	τ_0	ν_0	α_i
User-1	0.96 T	1.2 F	0.33
User-2	0.96 T	1.2 F	0.33
User-3	0.96 T	1.2 F	0.33
User-4	0.96 T	1.2 F	0.33

(b)

User (UBO)	τ_0	ν_0	α_i
User-1	0.96 T	1.16 F	0.28
User-2	0.96 T	1.16 F	0.28
User-3	0.96 T	1.16 F	0.23
User-4	0.96 T	1.16 F	0.36

(c)

User (FO/UBO)	τ_0	ν_0	α_i
User-1	1 T	1.02 F	0
User-2	1 T	1.02 F	0
User-3	1 T	1.02 F	0
User-4	1 T	1.02 F	0

distributed between 0 and these values. Since NO doesn't allow subcarrier overlapping, ν_0 begins from 1 for NO curves. On the other hand, overlapping in time is considered for all approaches.

It is shown that subcarrier overlapping techniques, UBO and FO overperform NO under the effect of time dispersive channels. The interesting result, though expected, is that the benefit gained by suppressing sidelobes in time domain with greater α values, is more than the expense of intentional ICI. This is particularly the case since sidelobes of RRC filter cause more interference than the edge part of subcarriers in multipath environments. If this comparison is done for greater α values, i.e., greater ν_0 values, the difference is seen more clearly. Because, edge parts of the subcarriers become smoother and the amount of interference due to the overlapping is decreased significantly.

In subcarrier overlapping scenarios, UBO provides more spectral efficiency than FO. Once it is thought with α-based scheduling, the subcarriers allocated for the worst-case users are near the

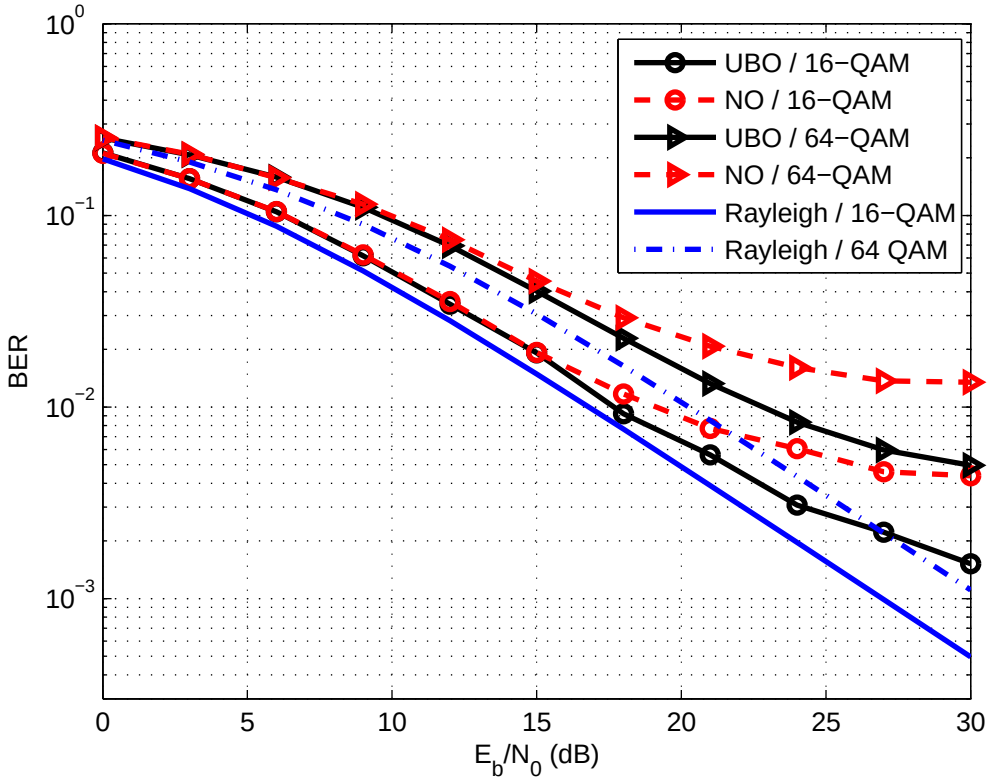

Figure 4.11 BER performance comparison of conventional NO and proposed UBO for different modulation orders ($\tau_{\text{rms}} = 2$ μs, $\nu_0 = 1.4$ and $\tau_0 = 1$).

subcarriers of best-case users. Therefore, more overlapping flexibility by maintaining desired SIR performance is obtained. Since, the user diversity becomes more clear in more dispersive channels in time, i.e., channels whose maximum τ_{rms} is greater, the advantage of UBO can be observed more obviously as shown in Figure 4.10 . In Table 4.1 required spacing and α parameters are given for UBO and FO where minimum desired SIR is 22 dB and maximum τ_{rms} of the channel is 2 μs. There are two options of parameter set to meet SIR demand. Since one of these parameter sets is same for both techniques, it is given in the same table on left hand side. User-4 is the one in the worst case and for UBO the greatest α, 0.36, belongs to that user as expected.

In order to show the projection of SIR gain on BER performance, Figure 4.12 and Figure 4.11 are also provided for the user in the worst case. In Figure 4.11, QAM symbols are transmitted with conventional NO and proposed technique UBO for $\tau_{\text{rms}} = 2$ μs, $\nu_0 = 1.4$ and $\tau_0 = 1$. The BER curves for the Rayleigh fading channel are also put as reference. In general, for identical QAM

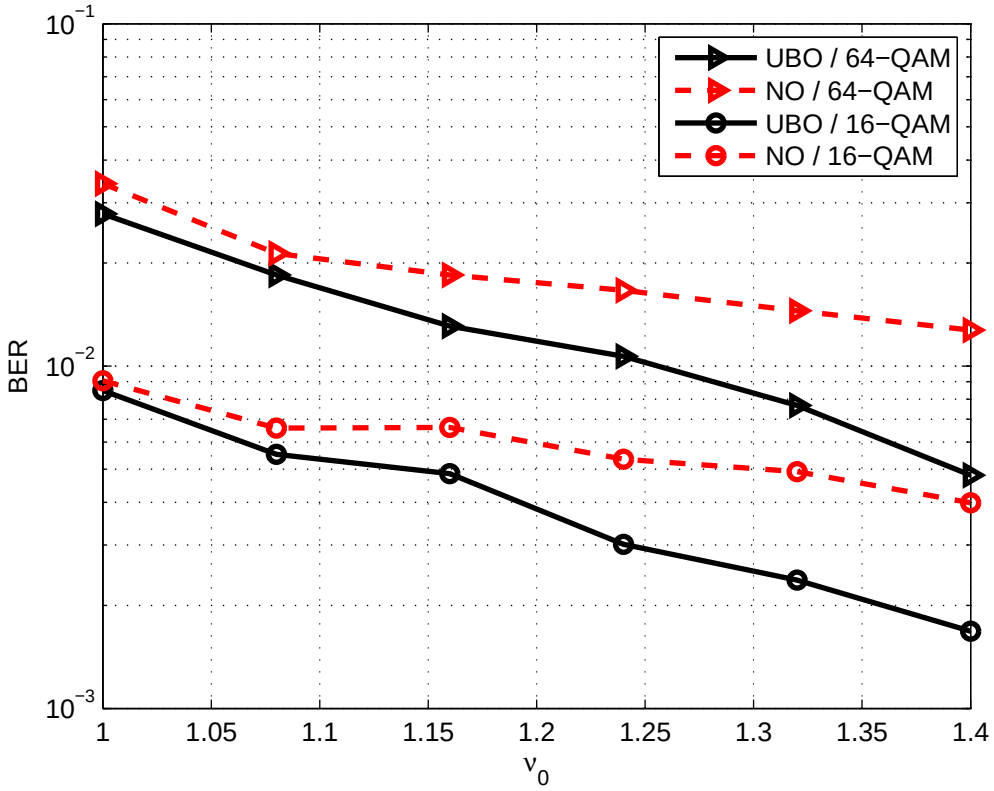

Figure 4.12 BER performance comparison of conventional NO and proposed UBO for different ν_0 values and modulation orders when SNR is 30 dB ($\tau_{\text{rms}} = 2$ μs, $\tau_0 = 1$).

modulation orders, UBO demonstrates a better BER performance as compared to NO. When the signal power becomes more dominant, the effect of the difference in SIR performance can be seen more obviously. Therefore, in order to provide the possible gain in spectrum efficiency, BER values of NO and UBO are given in Figure 4.12 for different ν_0 values when the SNR is 30 dB. Required subcarrier spacings for both technique can be compared and the gain in spectrum efficiency with UBO can be calculated for a desired BER. For example, if modulation is chosen as 64-QAM, while we can reach $10^{-2.5}$ BER for $\nu_0 = 1.15$ with UBO, same performance can be obtained when $\nu_0 = 1.3$ with conventional NO. Consequently, more than 10% spectrum is saved for this BER performance. More advanced optimization techniques may provide better α sets to improve this gain, but it is out of scope for this study.

4.5 Conclusion

In this study, a spectrally efficient user-aware intentional overlapping technique is presented for multicarrier schemes. While conventional approaches keep the minimum distance between neighboring symbols to prevent self interference, this study focus on to improve spectral efficiency by overlapping the symbols in time and frequency as long as the user in the worst case is satisfied. Although, the spectrum efficiency obtained with intentional overlapping may not be considered as a fundamental capacity gain, e.g., Shannon capacity, proposed technique provides an efficient usage of spectrum under practical channel facts. Unlike other intentional overlapping schemes, according to channel state information of each user, different RRC filters in terms of roll off factor are utilized in order to provide more overlapping flexibility. Consequently, in multi-user scenarios, proposed tecnique shows the best performance among the other multicarrier schemes.

In order to provide a more reliable and spectrum efficient system than presented technique, there are some issues that should be addressed. Implementation is definitely one of these issues, since the method does not fit the current fast implementation algorithms, e.g., FFT and polyphase network (PPN). Also, if $\nu_0\tau_0$ multiplication falls below 1, system becomes linear dependent which requires maximum likelihood sequence estimation (MLSE) type of techniques for perfect reconstruction which adds extra complexity to the receiver. Secondly, we focused on roll-off factor (α) based waveform design in this study. However, combining this technique with channel aware, α-based scheduling and interference cancellation algorithms would provide more efficiency in spectrum.

CHAPTER 5:

CONCLUSION

In this thesis, user-specific filter utilization is presented for multicarrier schemes. A novel procedure is followed unlike the conventional waveform design. Considering the facts of multi-user scenarios, pulse shaping filters whose time and frequency characteristics depend on the wireless channel of corresponding user are employed. Proposed technique is also used in designing a denser frame structure that uses spectral resources efficiently. Note that, proposed technique does not provide a fundamental capacity gain over Shannon capacity. Basically, multi-user diversity is exploited to improve spectrum efficiency. Symbols are overlapped in time and frequency domain, and more overlapping is achieved by using user-based filters.

As an extension of presented study, similar analysis can be performed considering different user requirements based on the applications that they are using. However, this study is confined to exploitation of user diversity in terms of wireless channels and extensions are left for future studies.

REFERENCES

[1] T. Yucek and H. Arslan, "A survey of spectrum sensing algorithms for cognitive radio applications," *IEEE Commun. Surveys Tutorials*, vol. 11, no. 1, pp. 116–130, 2009.

[2] J. Wang, M. Ghosh, and K. Challapali, "Emerging Cognitive Radio Applications: A Survey," *IEEE Commun. Mag.*, vol. 49, no. 3, pp. 74–81, Mar. 2011.

[3] H. F. Harmuth, "On the transmission of information by orthogonal time functions," *AIEE Transactions, Part I: Communication and Electronics*, vol. 79, no. 3, pp. 248-255, July 1960

[4] *Radio Broadcasting Systems; Digital Audio Broadcasting (DAB) to mobile, portable and fixed receivers*, ETSI - European Telecommunications Standards Institute EN 300 401 Std., Rev. 1.4.1, Aug. 2006.

[5] *Digital Video Broadcasting (DVB); Framing structure, channel coding and modulation for digital terrestrial television*, ETSI-European Telecommunications Standards Institute Std. EN 300 744, Rev. 1.4.1, Jan. 2001

[6] *Very high speed digital subscriber line transceivers 2 (VDSL2)*, ITU - International Telecommunication Union - T G.993.2 Std., Dec. 2011.

[7] *IEEE Standard for Information technology-Telecommunications and information exchange between systems Local and metropolitan area networks-Specific requirements Part 11: Wireless LAN Medium Access Control (MAC) and Physical Layer (PHY) Specifications*, IEEE 802.11 Std., 2012.

[8] M. L. Doelz, E. T. Heald, and D. L. Martin, "Binary Data Transmission Techniques for Linear Systems," *Proc. IRE*, vol. 45, pp. 656–661, May 1957.

[9] B. Saltzberg, "Performance of an efficient parallel data transmission system," *IEEE Trans. Commun. Technol.*, vol. 15, no. 6, pp. 805–811, Dec. 1967.

[10] R. W. Chang, "Synthesis of band-limited orthogonal signals for multichannel data transmission," *The Bell System Technical J.*, pp. 1775–1796, Dec. 1966.

[11] B. Farhang-Boroujeny, "OFDM versus filter bank multicarrier," *IEEE Sig. Proc. Mag.*, vol. 28, no. 3, pp. 92–112, 2011.

[12] G. Cherubini, E. Eleftheriou, and S. Olcer, "Filtered multitone modulation for very high-speed digital subscriber lines," *IEEE J. Select. Areas Commun.*, vol. 20, no. 5, pp. 1016–1028, June 2002.

[13] ——, "Filtered multitone modulation for VDSL," in *Proc. IEEE Global Telecommun. Conf. (GLOBECOM)*, vol. 2, Rio de Janeiro, Brazil, Dec. 1999, pp. 1139–1144.

[14] P. Amini, "Filtered multitone for slow fading and fast fading channels," *Ph.D. dissertation*, Dept. of Electrical and Computer Eng., University of Utah, May, 2013.

[15] A. Viholainen, T. Ihalainen, T. H. Stitz, M. Renfors, and M. Bellanger, "Prototype filter design for filter bank based multicarrier transmission," in *European Signal Processing Conference (EUSIPCO)*, Glasgow, Scotland, Aug. 2009.

[16] B. Hirosaki, "An orthogonally multiplexed QAM system using the discrete Fourier transform," *IEEE Transactions on Communications*, vol. 29, no. 7, pp. 982-989, July 1981.

[17] D. Chen, D. Qu, and T. Jiang, "Novel prototype filter design for fbmc based cognitive radio systems through direct optimization of filter coefficients," in *Proc. IEEE International Conference on Wireless Communications and Signal Processing (WCSP),*, Oct. 2010, pp. 1–6.

[18] B. Farhang-Boroujeny, "A square-root nyquist (M) filter design for digital communication systems," *IEEE Trans. Sig. Proc.*, vol. 56, no. 5, pp. 2127–2132, May 2008.

[19] Vahlin, Anders, and Nils Holte. "Optimal finite duration pulses for OFDM." Communications, IEEE Transactions on 44.1 (1996): 10-14.

[20] J. E. Mazo, "Faster-Than-Nyquist Signaling," *The Bell System Technical J.*, vol. 54, pp. 1451–1462, Oct. 1975.

[21] F. Rusek and J. Anderson, "The two dimensional Mazo limit," in *Proc. IEEE Int. Symp. on Information Theory (ISIT)*, Sep. 2005, pp. 970–974.

[22] F. Rusek and J. B. Anderson, "Successive interference cancellation in multistream faster-than-Nyquist signaling," in *Proc. Intl. Wireless Comm.and Mobile Computing Conf.* New York, NY, USA: ACM, 2006, pp. 1021–1026.

[23] A. Mishra, E. Rozner, S. Banerjee and W. Arbaugh, "Exploiting Partially Overlapping Channels in Wireless Networks: Turning a Peril into an Advantage," in *ACM/USENIX Internet Measurement Conference* 2005.

[24] A. Mishra, V. Shrivastava, S. Banerjee, and W. Arbaugh, "Partially overlapped channels not considered harmful," in *SIGMETRICS Perform. Eval. Rev. 34(1)* 2006.

[25] Z. Feng and Y. Yang, "How Much Improvement Can We Get From Partially Overlapped Channels?," in *Proceedings of IEEE WCNC* pp. 2957 2962, 2008.

[26] H. Liu, H. Yu, X. Liu, C. Chuah, P. Mohapatra, "Scheduling multiple partially overlapped channels in wireless mesh networks," in *in Proc. ICC* 2007.

[27] Z. E. Ankarali, A. Sahin, and H. Arslan, "Adaptive roll-off factor utilization in FMT-based FBMC burst structures," in *SDR Forum*, Washington DC, Jan. 2012.

[28] Z. E. Ankarali, A. Sahin, and H. Arslan, "Intentional-overlapping for multicarrier schemes based on user-specific filters," *Analog Integrated Circuits and Signal Processing*, pp. 1-8, 2013

[29] A. Sahin, I. Güvenç, and H. Arslan, "A Survey on Multicarrier Communications: Prototype Filters, Lattice Structures, and Implementation Aspects," *CoRR*, vol. abs/1212.3374, 2012.

[30] J. C. I. Chuang, "The effects of time delay spread on portable radio communications channels with digital modulation," *IEEE J. Select. Areas Commun.*, vol. SAC-5, pp. 879-889, June 1987.

[31] J.J. Mor, "The Levenberg-Marquardt algorithm: implementation and theory.," *Numerical analysis*, Springer Berlin Heidelberg, pp. 105-116, 1978.

APPENDICES

Appendix A: Acronyms

OFDM	orthogonal frequency-division multiplexing
DVB-T	Terrestrial Digital Video Broadcasting
DAB	Digital Audio Broadcasting
ADSL	Asymmetric Digital Subscriber Line
WLAN	Wireless Local Area Networks
WPAN	Wireless Personal Area Network
CR	Cognitive Radio
ICI	inter-carrier interference
ISI	inter-symbol interference
CIR	channel impulse response
MIMO	multiple input-multiple output
BS	base station
PA	power amplifier
RF	radio frequency
EVM	error vector magnitude
DFT	discrete-Fourier transformation
IFFT	inverse-fast Fourier transformation
RC	raised cosine
CP	cyclic prefix
PAPR	peak-to-average power ratio
QAM	quadrature amplitude modulation
OQAM	offset quadrature amplitude modulation
FFT	fast Fourier transformation

Appendix A (Continued)

RRC	root-raised cosine
CFO	carrier frequency offset
SIR	signal-to-interference ratio
FBMC	filter bank multicarrier
FMT	filtered multitone
SMT	staggered multitone
CMT	cosine-modulated multitone
PPN	polyphase network
SINR	signal-to-interference-and-noise ratio
PDF	probability density function
PO	partially overlapping
FTN	faster-than-Nyquist
RMS	root-mean-square
WSSUS	wide-sense stationary uncorrelated scattering
IIR	infinite impulse response
OFDP	Optimum finite duration pulse
PSWF	prolate Spheroidal wave function
CSI	channel state information
BER	bit-error rate

ABOUT THE AUTHOR

Zekeriyya Esat Ankarali received the B.Sc. (with honors) degree in Control Engineering from Istanbul Technical University (ITU), Turkey in 2011. He is currently working towards the Ph.D. degree with the Department of Electrical Engineering, University of South Florida, Tampa, FL. His research interests include Cognitive Radio, multicarrier waveform design and baseband signal processing in wireless communications.